Progression of Organic Reactions on Resin Supports Monitored by Single Bead FTIR Microspectroscopy

Bing Yan,*[,†] Jay B. Fell,[‡] and Gnanasambandam Kumaravel[§,||]

Department of Central Technologies, Combinatorial Chemistry Group, and Department of Oncology, Preclinical Research, Sandoz Research Institute, Sandoz Pharmaceuticals Corporation, East Hanover, New Jersey 07936-1080

Received July 24, 1996[⊗]

We report the time courses of five solid-phase reactions obtained using single bead FTIR microspectroscopy. This time-resolved information aided in the determination of the required reaction time, the nature of the solid-phase reaction, and resin property, effectively assisting in the initial phase of our combinatorial chemistry efforts. Our results showed that solid-phase organic reactions proceed faster than generally speculated. In addition, we have shown that reactions on the surface and in the interior of the bead occur at the same rate for reactions studied. The reaction on the TentaGel resin was shown to be not faster than reactions on Wang resin, suggesting that the diffusion of the substrate into polystyrene bead copolymerized with 1% divinylbenzene is not rate-limiting. Finally, the capability of obtaining IR spectra from the partial surface of a single bead demonstrated the femtomolar detection limit of single bead FTIR microspectroscopy.

Introduction

The birth of combinatorial chemistry[1] has revived the technology of solid-phase organic synthesis. Reactions carried out on insoluble resins differ from their counterparts in solution in many aspects such as the accessibility, microenvironment, specificity, and reactivity of reactant molecules.[2] It has been suggested that "polymer effects" such as steric hindrance, catalysis, site separation, and viscosity would alter reaction mechanisms.[3] Steric hindrance due to the rigidity of the polymer chains was attributed as the reason for improving the yield and the selectivity of a reaction catalyzed by a solid-supported reagent.[4] These effects may also affect the rate of reactions carried out on resin supports.

Some reports dealing with the reaction time courses of solid-phase peptide synthesis and organic synthesis include using UV-vis spectrophotometric method,[5a−d] IR on KBr pellet of ∼10 mg beads,[5e] titration using 100−200 mg of beads,[5f] and chromatographic analysis of the reaction mixture.[5g,h] These methods all have limitations in their sensitivity and the scope of application. They are particularly not suitable for monitoring the small-scale combinatorial synthesis. Rapid on-bead determination of the outcome of solid-phase reactions would obviate the tedious cleavage of intermediates for each analysis to facilitate both the transformation of known solution-phase reactions and the development of new solid-phase chemistry that does not have a current solution-phase counterpart. Accurate knowledge of the time required for a reaction step to reach completion is also important during the production of compound libraries on solid-phase as well as during reaction optimization.

In general, the kinetics of organic reactions on solid supports are far less understood than their counterparts in solution. The mobility of reactants inside the polymer micropores is restricted due to the high viscosity in the bead interior. The mobility of polymer-bound substrate is dependent on the extent of swelling as shown by electron spin resonance (ESR).[6] It has been postulated that polymer-supported reactions are often slower than those carried out in solution.[7] A thorough understanding of the kinetics of solid-phase organic reactions has long been hindered by the lack of sensitive and rapid analytical tools for the real-time probing of solid-phase reactions. Consequently, chemists involved in solid-phase synthesis find it difficult to determine how much time is required for a reaction to reach the steady-state. As a result, more time than necessary is often spent in carrying out solid-phase synthesis. Consequences from the prolonged reaction time are, for example, the susceptibility to side reactions and the reduced product yield.

We have previously developed single bead FTIR microspectroscopy (single bead IR), a sensitive and rapid method for real-time monitoring of solid-phase organic

† Department of Central Technologies.
‡ Combinational Chemistry Group.
§ Department of Oncology.
|| Present address: Versicor, Marlborough, MA 01752-1183.

⊗ Abstract published in *Advance ACS Abstracts,* October 1, 1996.

(1) (a) Jung, G.; Beck-Sickinger, A. G. *Angew. Chem., Int. Ed. Engl.* **1992**, *31*, 367. (b) Pavia, M. R.; Sawyer T. K.; Moos, W. H. *Bioorg. Med. Chem. Lett.* **1993**, *3*, 387−396. (c) Gordon, E. M.; Barrett, R. W.; Dower, W. J.; Fodor, S. P. A.; Gallop, M. A. *J. Med. Chem.* **1994**, *37*, 1385−1401. (d) Fruchtel, J. S.; Jung, G. *Angew. Chem., Int. Ed. Engl.* **1996**, *35*, 17−42. (e) Thompson, L. A.; Ellman, J. A. *Chem. Rev.* **1996**, *96*, 555−600. (f) DeWitt, D. H.; Czarnik, A. W. *Acc. Chem. Res.* **1996**, *29*, 114. (g) Still, W. C. *Acc. Chem. Res.* **1996**, *29*, 155. (h) Ellman, J. A. *Acc. Chem. Res.* **1996**, *29*, 132. (i) Armstrong, R. W.; Combs, A. P.; Tempest, P. A.; Brown, S. D.; Keating, T. A. *Acc. Chem. Res.* **1996**, *29*, 123. (j) Gordon, E. M.; Gallop, M. A.; Patel, D. V. *Acc. Chem. Res.* **1996**, *29*, 144.

(2) Challa, G. *J. Mol. Catal.* **1983**, *21*, 1−16. Leznoff, C. C. *Acc. Chem. Res.* **1978**, *11*, 327−333.

(3) Guyot, A. *Synthesis and Separations using Functional Polymers;* Sherrington, D. C., Hodge, P., Eds.; John Wiley and Sons Ltd.: New York, 1988; pp 1−42.

(4) Capillon, J.; Ricard, A.; Audebert, R. and Quivoron, C. *Polym. Bull.* **1985**, *13*, 185−192.

(5) (a) Merrifield, B. *Br. Polym. J.* **1984**, *16*, 173−178. (b) Garden, J., II; and Tometsko, A. M. *Anal. Chem.* **1972**, *46*, 216−223. (c) Gisin, B. F. *Anal. Chim. Acta* **1972**, *58*, 248−249. (d) Chu, S. S.; Reich, S. H. *Bioorg. Med. Chem. Lett.* **1995**, *5*, 1053−1058. (e) Mazur, S.; Jayalekshmy, P. J. *Am. Chem. Soc.* **1979**, *101*, 677−683. (f) Lu, G.-S.; Mojsov, S.; Tam, J. P.; Merrifield, R. B. *J. Org. Chem.* **1981**, *46*, 3433−3436. (g) Blanton, J. R.; Salley, J. M. *J. Org. Chem.* **1991**, *56*, 490−491. (h) DeWitt, S. H.; Kiely, J. S.; Stankovic, C. J.; Schroeder, M. C.; Reynolds Cody, D. M.; Ravia, M. R. *Proc. Natl. Acad. Sci. U.S.A.* **1993**, *90*, 6909−6913.

(6) Regen, S. L. *Macromolecules* **1975**, *8*, 689.

(7) Hodge, P. *Synthesis and Separations using Functional Polymers* Sherrington, D. C., Hodge, P., Eds.; John Wiley and Sons Ltd.: New York, 1988; pp 43−122.

S0022-3263(96)01416-8 CCC: $12.00

Scheme 1

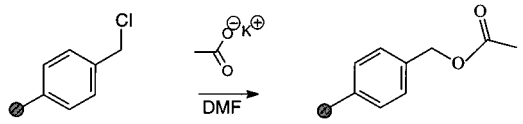

I

reactions.[8] In order to explore this technique for the elucidation of solid-phase reaction kinetics, we analyzed the IR spectrum of a single bead at various times after the initiation of a reaction. The quick and accurate acquisition of the time-resolved information on solid-phase synthesis aided the determination of the proper reaction time and the understanding of the properties of solid-phase reactions and the frequently-used resin supports.

Results and Discussion

I. Kinetics of an S_N2 Reaction on Merrifield Resin. The S_N2 reaction is an important class of reactions for the formation of C−O, C−S, C−N and C−C bonds. The mechanism of this reaction is concerted, involving a trigonal bipyramid transition state. The association of the reactant with the solid support could affect the concerted reaction pathway and therefore the rate of the reaction. It is conceivable that a solid-phase S_N2 reaction as the acetylation of the chloromethyl polystyrene resin shown in Scheme 1 might occur at a much slower rate compared with that in solution. It is not surprising that these reactions were often run for extended times (such as 24 h in reference 9). We monitored the time course of this reaction directly on a solid support in order to understand the effect of a polymer carrier on the reaction. A drop of reaction suspension was removed from the reaction vessel at various times after the initiation of the reaction. The tiny amount of resin beads in the drop was first washed with DMF (three times), then methanol (three times) and finally vacuum dried (15 min). A few beads from each time point were transferred to a NaCl plate under the microscope and the IR spectrum of a single flattened bead[8b] was taken (Figure 1). The time course of this reaction obtained by taking data from Figure 1 is shown in Figure 2. An estimated pseudo-first-order rate constant of 5.0×10^{-4} s^{-1} was obtained by fitting with eq 4 derived in the Experimental Section. In order to compare this reaction rate with the rate of the second-order reaction in solution, we calculated the $t_{1/2}$ for the solid-phase reaction as 23 min. The rate of this reaction is much faster than those of similar reactions in solution ($k = 10^{-3}-10^{-2}$ s^{-1} M^{-1} or $t_{1/2} = 170-1700$ min).[14] Low solubility of the starting material potassium acetate in the reaction solvent DMF is common to both solid-phase and solution-phase reactions. Mechanistically, the nucleophile must approach the center at which substitution occurs in the rate-determining step; therefore more and larger substituents (such as the polymer backbone in a solid supported reaction) on the substrate decrease the rate.[15] However, the reactant may be concentrated within the polymer bead, and this high local concentration may play a role in accelerating the reaction.

II. Esterification Reactions on TentaGel Resins. The resin backbone determines the solvation and swelling property of the polymer. The extent of swelling of the resin in turn affects the diffusion rate of the starting material and the reactivity of the bound substrate.[7] Esterification reactions have been previously studied on Wang resin.[8a] We reanalyzed the published data[8a] using

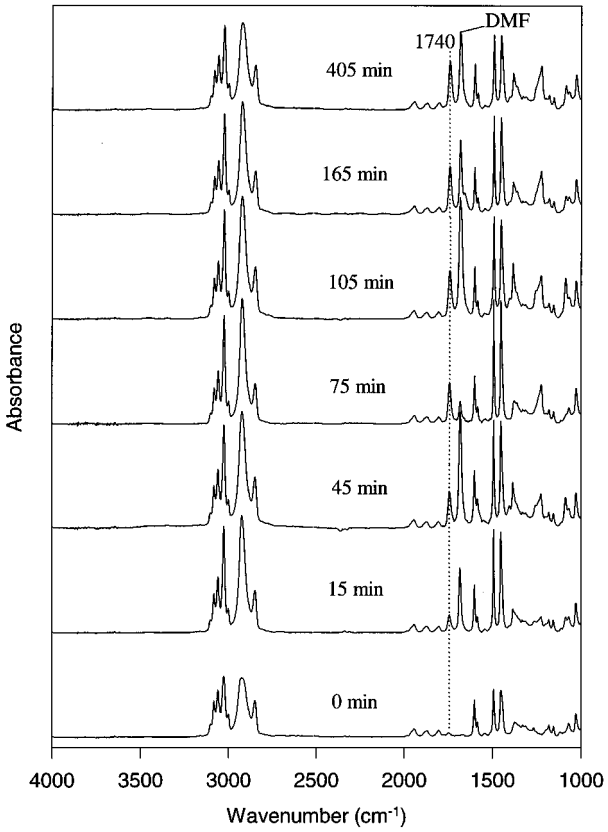

Figure 1. IR spectra from a single bead taken at specified times during the course of reaction I. The absorbance spectra were taken as described in the Experimental Section. The carbonyl peak at 1740 cm^{-1} is highlighted with the dotted line. The peak at 1658 cm^{-1} is from residual solvent DMF. The irregular intensity of this peak may be due to the insufficient drying and the different solvent-adsorbing property of the individual bead. See Figure 2 for the kinetic analysis and the rate constant.

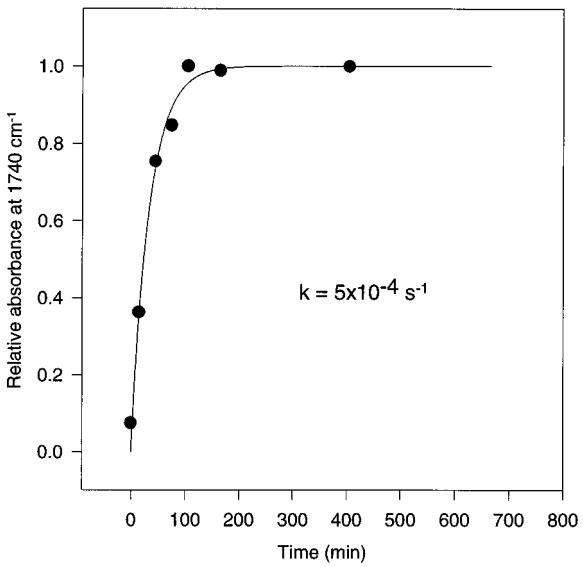

Figure 2. The time course of reaction I. The progression of the absorbance at 1740 cm^{-1} as shown in Figure 1 was plotted against time. The solid line is the best fit time course according to eq 4 with $k = 5 \times 10^{-4}$ s^{-1}.

(8) (a) Yan, B.; Kumaravel, G.; Anjaria, H.; Wu, A.; Petter, R.; Jewell, C. F., Jr.; Wareing, J. R. *J. Org. Chem.* **1995**, *60*, 5736−5738. (b) Yan, B.; Kumaravel, G. *Tetrahedron* **1996**, *52*, 843−848.

Scheme 2

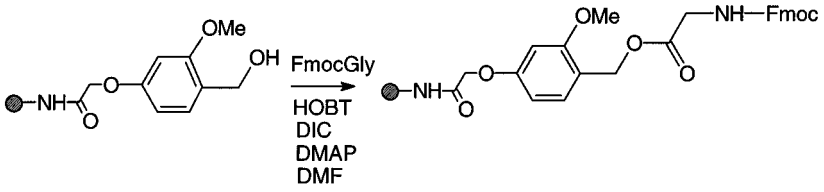

II

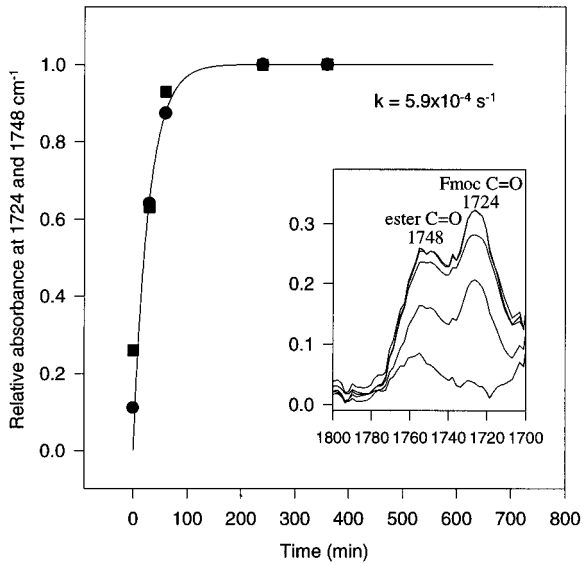

Figure 3. The IR spectra and the time course for reaction II. Reaction conditions and kinetics analysis are described in the Experimental Section. Spectra were taken on the whole bead without flattening in this case because flattening crushed the TentaGel resin bead. In the order of the increased intensity at 1724 cm^{-1}, IR spectra from a single bead at 0, 0.5, 1, 4, and 6 h after the initiation of reaction II (Scheme 2) were plotted in the insert. These spectra were normalized making the resin band at 1950 cm^{-1} of equal intensity. Two carbonyls were formed in this reaction: an ester carbonyl at 1748 cm^{-1} and a Fmoc at 1724 cm^{-1}. The absorbance at 1724 and 1748 cm^{-1} are plotted against time. The solid line is the best fit time course according to eq 4 with $k = 5.9 \times 10^{-4}$ s^{-1}. Circles represent the intensity of the Fmoc carbonyl, and squares represent that of the ester carbonyl.

eq 4 and obtained a rate constant of 5×10^{-3} or a $t_{1/2}$ of 3 min. TentaGel resins differ from other polystyrene based resins in that a poylethylene glycol spacer is placed between the polymer backbone and the reactive sites. In theory this separation places the reactive site in a more "solution-like" environment. If this is true the polymer backbone would have less of an effect on the reaction kinetics. The time course of reaction II (Scheme 2) carried out on TentaGel S AC can be followed by simultaneously monitoring the ester carbonyl at 1748 cm^{-1} and the Fmoc carbonyl at 1724 cm^{-1}. The progression of intensities of these two bands is shown in the inset of Figure 3. A rate constant of 5.9×10^{-4} s^{-1} was calculated by fitting the reaction time course to eq 4 (Figure 3). The $t_{1/2}$ for this reaction is 20 min. The time course of an esterification reaction on Wang resin[8a] is estimated to be 5×10^{-3} s^{-1} fitted with the same equation. This corresponds to a $t_{1/2}$ of 3 min. The reaction carried out on Wang resin is even faster. The comparison is not very quantitative since the two reactions are not exactly the same. However, the reaction on Tentagel resin is slower, indicating that the polyethylene oxide spacer in TentaGel resin exhibited no evident

Scheme 3

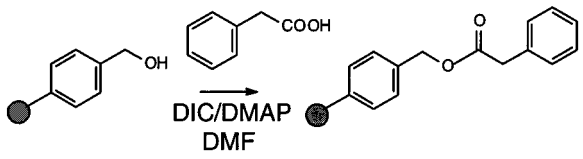

III

improvement on reaction rate for the reaction studied. This suggests that the diffusion of the substrate into the polystyrene backbone of the bead is not rate-limiting for polystyrene bead copolymerized with 1% DVB. As exemplified here, time-resolved single bead IR provides a useful tool for monitoring the effect of different resin structures on reaction rate and an aid in the selection of solid support.

III. Comparison of Reaction Kinetics on the Surface with That in the Interior of a Single Bead. It is known that more than 99% of the reactive sites on a resin bead are in the microporous interior of the bead.[7] Resin-supported reactions occur mostly in the interior of the bead because the yield of the cleaved product eventually will reach a level which is comparable to the loading of the bead. Reactions carried out in the interior of solid supports were speculated to be diffusion controlled.[3,7] Presumably, if diffusion of reactant or reagent molecules into and out of the polymer bead is slower than the reaction rate, the reaction will occur initially on the outer shell of the bead. However, no experimental data have ever been reported to test this hypothesis. We examined this hypothesis experimentally for the first time by comparing the reaction rate on the surface of the bead and in the bead interior using single bead IR. An attenuated total reflection (ATR) objective was placed in contact with a single bead, and the IR spectrum of compounds on the partial surface of the bead was taken. The progression of the IR intensity of the product at various reaction time points reflects the chemical reaction rate on the surface of the bead. With a regular microscopic objective in the transmission mode, the IR spectrum of the whole bead was obtained. Since >99% of the IR intensity is from materials in the interior of the bead,[6] the progression of IR intensity of the product measured this way actually reflects the chemical reaction taking place in the interior of a bead. The bead-flattening technique[8b] was used for measuring the whole bead spectrum. The sampling volumes on a single bead by the two methods are illustrated in Figure 4.

Reactions III and IV are esterifications (Scheme 3 and 4). Reaction V (Scheme 5), a nucleophilic substitution reaction, proceeds with the introduction of an ester moiety. The intensity of the ester carbonyl stretch at 1738 cm^{-1} increases during the time course for all of these reactions. Figure 5 shows single-bead IR spectra taken at various times after the initiation of reaction III. Intensity of the 1723 cm^{-1} band increases with time and

Figure 4. Two-dimensional drawing of the sampling volumes for the surface experiment using ATR mode, and the whole bead experiment using transmission mode. On the left, the cross-section of a bead in an ATR experiment is shown. The dark area shows the cross-section of the sampling volume. In the ATR mode, an ATR objective is in contact with a bead. Please note that although not shown in the figure, the bead may be slightly flattened when in contact with the ATR objective. The IR beam penetrates into the partial surface and is reflected with attenuated intensity. On the right, the cross-section of a flattened bead is shown. IR beam transmits the whole bead, and the sampling volume is the whole bead.

Scheme 4

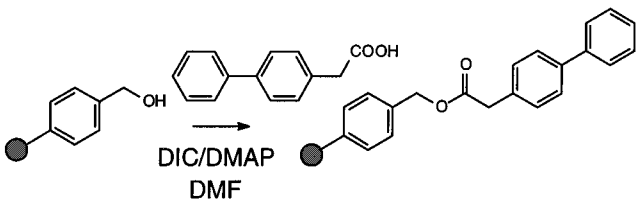

IV

that of 3445 cm^{-1} band decreases simultaneously. The time-dependent changes in the intensity at 1738 cm^{-1} recorded from the surface of a bead and from the bead interior were plotted in Figure 6 A−C (circles are for the surface and squares for the bead interior). Pseudo-first-order rate constants for reactions III, IV, and V are 4.6 $\times 10^{-3}$, 6.3 $\times 10^{-3}$, and 6.0 $\times 10^{-4}$ s^{-1}. For these reactions, there is no discernible difference in the reaction rate at the bead surface and in the interior of the bead. We also compared reaction rates on the bead surface and in the bead interior for a reaction reported earlier (reaction II in ref 8a). The reaction proceeded in the same rate (2.3×10^{-3} s^{-1}) on the bead surface and in the bead interior. Therefore, the rate of progression of these reactions inside the bead is apparently similar to that observed for reactions on the surface. Although the diffusion of organic compounds into the interior of a resin bead is slower than the diffusion in solution as observed by Ford et al.,[16] the effect of the polymer structure on the reaction rate is complex. In a microscopic view, the bimolecular rate constant is proportional to diffusion constants of both molecules and the distance of separation of the molecular centers.[17] High viscosity in the bead interior may restrict the diffusion, but also reduce the distance of separation between molecules causing an overall rate increase. These two polymer effects may counter-balance each other. Although no difference in reaction rates on the bead surface and in the bead interior was found for reactions we studied, the diffusion rates of much bulkier substrate and the charged species into the micropores of the bead remain to be examined.

IV. Femtomolar Detection Limit. Both biological assays and synthesis have been driven to the direction of miniaturization and high-capacity. As an analytical method for the resin bead, a high sensitivity is desired. Previously, we obtained IR spectra of a single bead on which the loading is approximately 500 pmol. (Wang resin bead, 1.05 mmol/g, ~100 μm diameter). In this work, we also applied the ATR microspectroscopy to analyze a single bead. The sampling volume in this case is a small area (Φ 41.7 μm) from the surface of a bead with a penetration depth of ~2 μm depending on the wavelength of the incident beam. The lowest detectable signal of the product is when the product yield is 5%.

Scheme 5

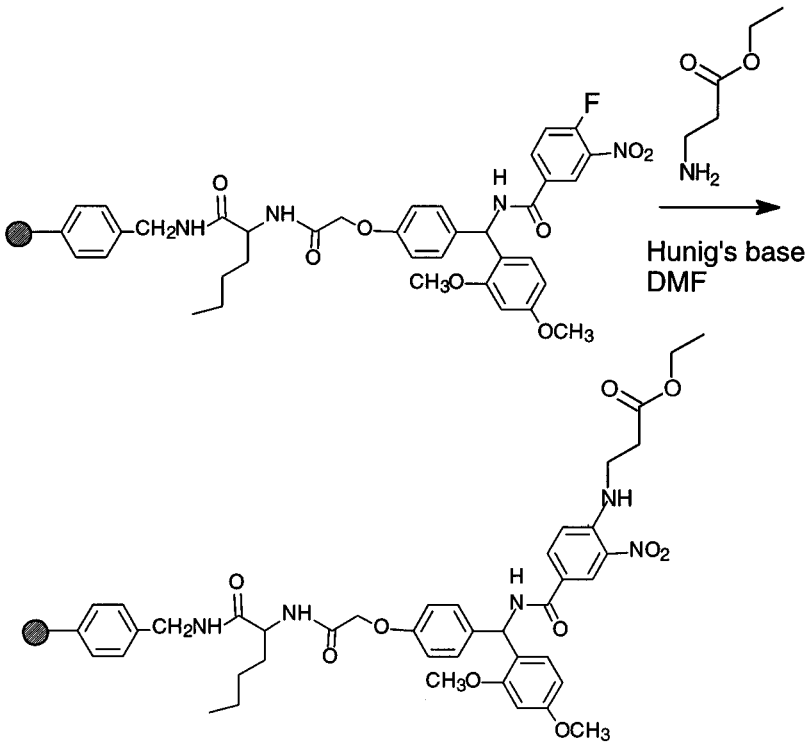

V

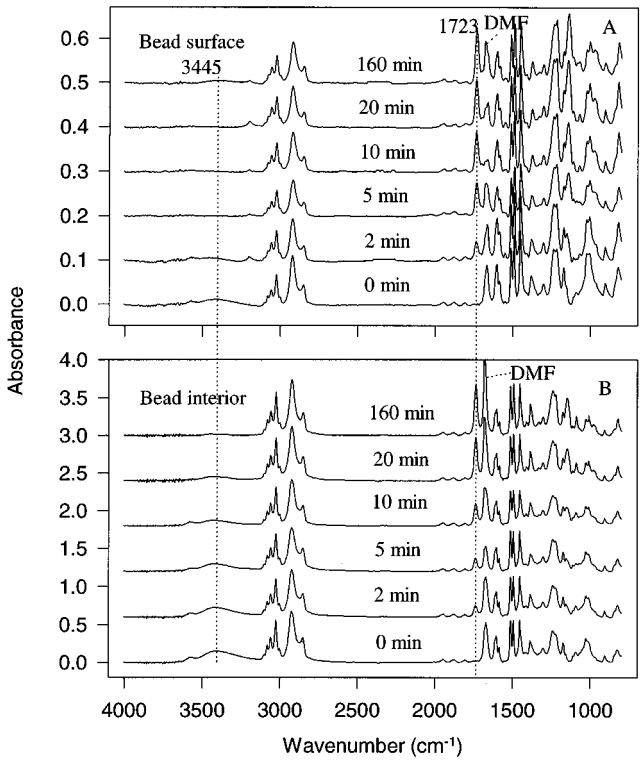

Figure 5. IR spectra from a single bead taken at specified times during the course of reaction III. Reaction conditions and analysis procedure are described in the Experimental Section. Spectra taken from a partial surface of a single bead are shown in A and from the whole bead in B. The sampling volumes are shown in Figure 4. The amount of compound sampled is calculated to be 130 fmol (see Experimental Section) for the surface measurement and ~500 pmol for the whole bead experiments. IR absorbance bands attributable to disappearing hydroxyl group at 3445 cm^{-1} and the emerging carbonyl group at 1738 cm^{-1} are highlighted with the dotted lines. Data analysis and the derived rate constants are shown in Figure 6A.

Then the detection limit currently achieved by us is 500 $\times$ 0.0052 $\times$ 0.05 = 130 fmol or 1.3 $\times$ 10^{-13} mol based on the detection of carbonyls. This is only an estimate considering errors inherent in IR measurement. This amount is ~1/3850 of the total loaded materials on a single bead. This result demonstrates that single bead IR is a highly sensitive technique suitable for future challenges from miniaturized samples.

Conclusion

The rates of solid-supported reactions have long been speculated to be much slower than those of similar reactions in solution. Without knowing the actual reaction kinetics, synthetic chemists generally have used longer reaction times on solid support than are necessary. The prolonged reaction not only wastes manpower and time, but also causes unnecessary side-reactions and a reduced product yield. We have demonstrated the ability to follow reaction kinetics with single bead IR, making this technique invaluable for the development of solid-supported reactions. Several significant findings were uncovered during the course of this work. Contrary to popular belief, we have shown that solid-phase reactions are not always slower than solution reactions and they can even have a greater rate. We have also shown that the rates of reaction on the surface of a bead and in the microporous interior of a bead do not differ greatly for the reactions studied by us. By comparing the rates of reactions run on TentaGel and Wang resin we have discovered that the reaction on TentaGel was not faster than a similar reaction on Wang resin, suggesting that the diffusion of the substrate into polystyrene bead copolymerized with 1% DVB is not rate-limiting. Our success in obtaining an IR spectrum from the partial surface of a bead also demonstrated that single bead IR is a highly sensitive method with a femtomolar detection limit.

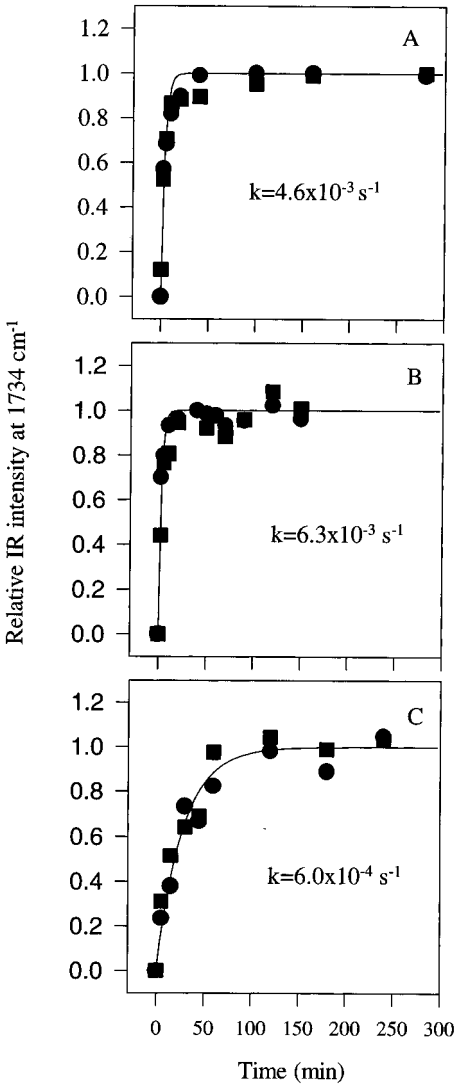

Figure 6. Comparison of the time courses of Reactions III–V on the bead surface and in the bead interior. The progressions of the absorbance at 1738 cm^{-1} from IR spectra taken on the bead surface and in the bead interior as in Figure 5 were plotted against time for Reactions III, IV, and V in panels A, B, and C. Absorbances were normalized to make a resin peak at 1945 cm^{-1} equal intensity for comparison. Circles are from spectra taken from the bead surface, and squares from the whole bead. Lines are best fit time courses according to eq 4 with k = 4.6 $\times$ 10^{-3}, 6.3 $\times$ 10^{-3}, and 6.0 $\times$ 10^{-4} for reactions III, IV, and V.

Experimental Section

Materials. The polymer matrix for all resins used in this work is the copoly(styrene-1%-divinylbenzene (DVB)). Wang resin[9] (*p*-(benzyloxy)benzyl alcohol, 1.05 mmol/g, 200–400 mesh) was purchased from Midwest Bio-tech (Fishers, IN). The

(9) Wang S. S. *J. Am. Chem. Soc.* **1973**, *95*, 1328–1333.

swelling volume of this resin in dichloromethane is 2−4 mL/g. The loading of this resin is calculated from the substitution level of the precursor resin by manufacturer. TentaGel S AC resin[10] (loading 0.2−0.25 mmol/g, 200−400 mesh) was purchased from Rapp Polymere GmbH (Tübingen, Germany). This resin features a crosslinked polyethylene glycol (PEG) spacer on a copoly(styrene-1%-DVB) matrix. The typical chain length of PEG is 68 ethylene oxide units giving an average molecular mass of 3000 Da. Due to the spacer effect of PEG, the reactive sites located at the end of the spacers are totally separated from the polystyrene backbone and completely solvated. Because of this quasihomogeneous behavior the resin shows high diffusion and sorption, and kinetic rates are expected to be in the same order as in solution. Since PEG content of TentaGel is up to 70−80% (w/w), the PEG dominates the physical−chemical behavior of the resin and makes it different from other resins used in this work. In this resin, a -OCH_2-CH_2NH- unit is linked to PEG spacer via a ether linkage and linked to the reactive group (Scheme 2) via an amide linkage. This resin is gelatinous and swellable in organic solvent as well as in aqueous systems. The swelling volume is nearly constant (4.25−5.7 mL/g) for water, MeOH, dichloromethane, DMF, MeCN, and THF. Merrifield resin[11] (chloromethylpolystyrene-1% DVB, 200−400 mesh) was purchased from Aldrich (Milwaukee, WI). The swelling volume of this resin in dichloromethane is 5.9−9.0 mL/g. The loading was calculated through elemental analysis of Cl by manufacturer. Rink amide AM resin[12] (4-(2′,4′-dimethoxyphenyl-Fmoc-aminomethyl)-phenoxyacetamido-norleucylaminomethyl resin, 200−400 mesh, 0.4−0.6 mmol/g) was purchased from NovaBiochem (San Diego, CA). The loading of this resin was calculated by photometric determination of the Fmoc-chromophore librated upon treatment with piperidine/DMF by manufacturer.

Solid-Phase Reactions. Reaction I. This is an S_N2 reaction in which the oxygen of the anionic acetate attacks the carbon center in the CH_2Cl group (Scheme 1). The chloride anion leaves and the acetate anion binds to the polymer in a concerted manner. Reaction was carried out on 1.0 g of Merrifield resin in DMF at 85 °C as described by Wang.[13] A drop of resin suspension was taken at specified times and subjected to a sequence of washing with DMF (three times), methanol (three times), and drying under vacuum (15 min). The FTIR microspectroscopy analysis procedure will be described in the next section.

Reaction II. This reaction was carried out on a TentaGel S AC resin. This esterification reaction (Scheme 2) took place in a "solution-like" microenvironment (see the description of TentaGel S AC resin). To make the Fmoc-Gly anhydride, diisopropylcarbodiimide (DIC, 310 μL, 2 mmol) was added to a DMF (2 mL) solution of Fmoc-Gly (590 mg, 2 mmol). This mixture was stirred at room temperature (rt) for 10 min. This anhydride solution was added to a suspension of TentaGel S AC (2.25 g, 0.24 mmol/g) in DMF (20 mL). 1-Hydroxybenzotriazole (HOBT, 370 mg, 2.4 mmol) and 4-(*N*,*N*-dimethylamino)pyridine (DMAP, 240 mg) were added to the mixture. The suspension was stirred at room temperature, and samples were taken at specified times.

Reactions III−V. Reactions III and IV are esterification reactions on Wang resin (Scheme 3 and 4). However, two starting materials differ in their size which may contribute to the different steric interactions entering the micropores of the bead. For each of reactions III and IV, Wang resin (1.0 g, 1.05 mmol/g) was suspended in DMF (2 mL). Phenylacetic acid, or 4-phenylphenylacetic acid (10 equiv) was treated with DIC (5 equiv) in DMF (2 mL) for 5 min, and this mixture was added to the resin suspension. DMAP was dissolved in DMF and added to the resin suspension. Reaction V is a nucleophilic aromatic substitution reaction (Scheme 5) on a bulkier polymer linked molecule which was made from Rink amide AM resin as previously described.[8b] For reaction V (Scheme 5), the starting resin (500 mg) was suspended in DMF (2 mL). β-Alanine ethyl ester hydrochloride (10 equiv) was added to the resin suspension followed by the addition of Hunig's base (20 equiv). Argon was bubbled through the resin suspension. For all reactions, samples were taken at specified times, washed three times with DMF and then three times with methanol, and vacuum dried.

FTIR Microspectroscopy. All spectra were collected on a BIO-RAD, FTS-40 spectrophotometer coupled with a UMA-300 IR microscope, using a SPC-3200 data station. The microscope is equipped with a 36X Cassegrain objective and liquid nitrogen-cooled mercury−cadmium−Telluride (MCT) detector. In the view mode the total visual magnification is 360X, which aided in locating a single bead. The transmission mode was used for the whole bead measurements.

A well polished NaCl window was used to collect the background spectrum. A few resin beads were then put on the NaCl window. Using the view mode and the X-Y platform of the microscope, the incident radiation was focused on a single resin bead. The diameter of the individual bead was measured under the microscope. Data were collected with 4 wavenumber resolution. Sixty-four scans were averaged.

The IR spectra of the bead surface was collected on a Magna-IR System 550 coupled with a Nic-Plan microscope with a Germanium attenuated total reflection (ATR) objective (Spectra-Tech Inc. Shelton, CT).

Kinetics Analysis. We analyzed kinetics data based on the following rationalizations. For reaction: Bead + A → B, the reaction rate is proportional to θ, the adsorbed fraction of molecule A, and $[S] = [S]_0 - [B]$, [S] is the fraction of the free reactive sites in bead and the initial fraction of free reactive sites, $[S]_o$, is 1.0. The rate of a solid-phase reaction

$$dB/dt = k(1 - [B])\theta \quad (1)$$

where $\theta = K[A]/(1 + K[A])$, $K = k_a/k_d$ is the adsorption equilibrium constant, k_a and k_d are the adsorption and desorption constants, and [B] is the fraction of the product. Equation 1 becomes

$$dB/dt = kK([A]_o - [B])(1 - [B])/\{1 + K([A]_o - [B])\} \quad (2)$$

In cases that reactant molecules can significantly adsorb onto bead ($k_a \gg k_d$) and the reactant is in large excess, $K([A]_o - [B]) \gg 1$, therefore

$$dB/dt = k(1 - [B]) \quad (3)$$

or

$$[B] = 1 - e^{-kt} \quad (4)$$

In this bimolecular reaction, reactant A is always in large excess. The overall reaction appears as a pseudo-first-order reaction, and the rate is limited by the reactivity of the starting materials and steric accessibility of reactants as reflected by the rate constant k. This is an empirical equation which fits experimental data well (see Figure 2, 3, and 6). The processes involved in the solid-phase reaction are far more complicated. The development of an equation accounting for all the solid-phase adsorption, reaction, and interaction processes is not the intention of this work.

Acknowledgment. We thank Professor William P. Jencks and Dr. Emil Fu for critical reading of the manuscript, and Bob Simler from Spectra-Tech for assistance in ATR FTIR microspectroscopy measurements.

JO961416R

(10) Bayer, E. *Angew. Chem., Int. Ed. Engl.* **1991**, *30*, 113−129.
(11) Merrifield, R. B. *J. Am. Chem. Soc.* **1963**, *85*, 2149−2154.
(12) Rink, H. *Tetrahedron Lett.* **1987**, *28*, 3787−3790.
(13) Wang, S.-S. *J. Org. Chem.* **1975**, *40*, 1235−1239.
(14) Shinoda, K.; Yasuda, K. *J. Org. Chem.* **1991**, *56*, 4081−4086.
(15) (a) Streitwieser, A., Jr. *Solvolytic Displacement Reactions*; McGraw-Hill: New York, 1962; p 13. (b) Cook, D.; Parker, A. *J. Chem. Soc. B* **1968**, 142.
(16) Ford, W. I.; Perigasany, M.; Spivey, H. O. *Macromolecules* **1984**, *17*, 2881−1886.
(17) Hammes, G. G. *Principles of Chemical Kinetics*; Academic Press: New York, 1978.